

PHASE STEERING AND FOCUSING BEHAVIOR OF ULTRASOUND IN CEMENTITIOUS MATERIALS

Shi-Chang Wooh and Lawrence Azar
Department of Civil and Environmental Engineering
Massachusetts Institute of Technology
Cambridge, MA 02139

INTRODUCTION

Deterioration of civil infrastructure system (CIS) raises not only safety issues but also socio-economic concerns. In order to meet the high demand of structural condition assessment and health monitoring, development of quick, reliable and accurate NDE methods became critical issues recently. Compared to metal structures, NDE for cement-based materials is still premature and requires further development.

Concrete structures, which are the popular basic building blocks of civil infrastructure systems, degrade with time due to a variety of physical and chemical processes. Composition of cement-based materials is complex, making it difficult to evaluate their structural conditions. In particular, it is challenging to use ultrasonic techniques to assess these materials primarily because concrete is naturally porous, inhomogeneous, highly attenuative and scatters ultrasound. More importantly, it is required to scan large area quickly.

Compared to the static nature of conventional transducers, phased arrays provide dynamic capabilities. These arrays, consisting of multiple elements excited at predetermined times, can be used to steer and focus ultrasonic beams dynamically. Low frequency phased array transducers may enjoy the merits of less labor-intensive operations, reduced inspection time, increased field of view, and improved signal to noise ratios. More detailed description can be found in the companion paper [1] published elsewhere in this volume. In this paper, we focus on showing the merits of focusing over steering in the near field.

Quality of beam steering and focusing can be characterized by the feature "beam directivity," defined by the distribution of pressure as a function of azimuthal angle. A phased array developed for assessing concrete structures has an inherently large aperture size due to the requirement of utilizing low frequency ultrasound. This results in a large *near field* or "dead zone" where the quality of beam steering is very much deteriorated.

Simulation studies show that focusing in the near field combined with steering greatly improves the near field directivity and reduces this dead zone. It is also shown that

the characteristics of the focused beam approaches that of steering when the focal spot is located in the far field. This phenomenon allows for efficient full field assessment of concrete structures. The simulation results agree well with experimental measurements, as shown in the companion paper [1].

OPTIMIZATION LIMITATIONS OF BEAM STEERING FOR CONCRETE

Sectorial diagnostic images are usually constructed by sweeping an ultrasonic beam throughout the area of interest and transforming the return signals into an image. This requires phase steering that is accomplished by sequentially pulsing the array elements.

The analytical pressure distribution regarding beam steering was previously derived by Wooh and Shi [3,4]. This analytical model is crucial in resolving the key parameters for these arrays. By analyzing the directivity patterns, beam steering characteristics were studied and optimum transducer parameters were determined. The fundamental transducer parameters studied include frequency (f), the element width (a), the center-to-center spacing of the elements (d), the number of elements (N), the total aperture dimension (D), and the elevation dimension (L).

It was concluded from this study that increasing N greatly improves the beam steering characteristics and also suppresses other detrimental effects. At the same time, increasing d improves the sharpness of the beam, up to a critical value. It is therefore desirable to use the largest number of elements spaced by the maximum allowable distances. This immediately poses a problem since it requires increased overall dimension, resulting in bulky transducers. More importantly, high values of these parameters increases transition zone that separates the near field from the far field of the array.

$$Z_{TR} \approx \frac{D^2 - \lambda^2}{4\lambda} . \quad (1)$$

For linear arrays, maximum allowable inter-element spacing without introducing spurious grating lobes is given [5] as

$$d_{\max} = \frac{\lambda}{1 + \sin(\theta_s)_{\max}} \frac{N - 1}{N} , \quad (2)$$

where λ is the wavelength of the acoustic medium and $(\theta_s)_{\max}$ is the required maximum steering angle. For large N and a , and assuming $D^2 \gg \lambda$, $(\theta_s)_{\max} = 90^\circ$, d_{\max} approaches $\lambda/2$ so that the overall dimension becomes $D \approx Nd$. Therefore, the transition zone can be expressed in terms of N as

$$Z_{TR} \approx \frac{N^2 \lambda}{16} . \quad (3)$$

For concrete, this transition can be significantly increased. For example, wavespeed of sound in a well-cured concrete can be in the range of 4,000 km/sec. If the transducer parameters are chosen such that $N = 16$ and $f = 100$ kHz, then the wavelength λ becomes approximately 4 cm and the corresponding optimum inter-element spacing is approximately

$\lambda/2 = 2 \text{ cm}$. With this design, the transition zone calculated from eq. (3) is 64 cm. Considering the fact that signals returned from this zone is unstable, this area beneath the transducer can be considered as unusable or “dead” zone, making it unattractive. This paper deals with an approach to remedy this problem by reducing the transition zone.

DYNAMIC FOCUSING AND THE PRESSURE FIELD

If targets within the near field of the array aperture are imaged, that is, at distances less than Z_{TR} , then focusing may be employed to increase the system resolution. In order to explain how focusing improves the resolution over steering, it is very critical to understand the behavior within this transition zone.

Focusing of the transmitted beam is accomplished by combining a parabolic timing relationship with a linear one to produce a beam which is focused at a given range and propagated at a specific azimuthal angle. The following generalized focusing formula was derived to compute the required time delays:

$$t_n = \frac{F}{c} \left\{ \left[1 + \left(\frac{\bar{N}d}{F} \right)^2 + \frac{2\bar{N}d}{F} \sin \theta_s \right]^{1/2} - \left[1 + \left(\frac{(n - \bar{N})d}{F} \right)^2 - \frac{2(n - \bar{N})d}{F} \sin \theta_s \right]^{1/2} \right\} \quad (4)$$

for any number of elements N , where t_n is the required time delay for element $n = 0, \dots, N - 1$, $\bar{N} = (N - 1)/2$, d is the center-to-center spacing between elements, F is the focal length from the center of the array, θ_s is the steering angle from the center of array, and c the wavespeed. This generalized focusing time delay formula is valid for any number of array elements (even or odd). Furthermore, by eliminating the constant t_0 , the formula guarantees positive time delays which do not have to be larger than necessary.

The analytical pressure distribution for the beam focusing was obtained as [4]:

$$p(r, \theta, t) = \left(\frac{p_0}{r} \right)^{\frac{1}{2}} \frac{\sin \left(\frac{ka \sin \theta}{2} \right)}{\frac{ka \sin \theta}{2}} \exp \left(-\frac{jka \sin \theta}{2} \right) \left(\sum_{n=0}^{N-1} \exp[j(An + Bn^2)] \right) \exp[j(\omega t - kr)] , \quad (5)$$

where k is the wave number, ω is the angular frequency, p_0 is a function of k , j is the unit imaginary number, and

$$A = \frac{c(N - 1)}{2F \tan^2 \theta_s} \Delta \tau_0^2 - \omega \Delta \tau_0 + kd \sin \theta , \quad (6)$$

$$B = \frac{c \Delta \tau_0^2}{2F \tan^2 \theta_s} .$$

This expression is useful for studying the far field characteristics of the beam focused beyond the transition range, as discussed later. However, it should be noted from eq. (5) that the pressure distribution for beam focusing can not be simplified into a closed form. This means that the analytical method is not possible; instead, the numerical method to simulate the acoustic field is desirable and powerful.

Numerical Simulation

A numerical simulation program was developed to attain directivity and image pressure profiles for ultrasonic linear phased arrays. This software simulates wave propagation fields for either steering or focusing, in both the near and far fields, and produces directivities at any specified distance. The pressure along the steered direction when steering or focusing was also simulated.

The simulation is based upon Huyghen's principle, which states that wave interactions can be analyzed by summing the phases and amplitudes contributed by a number of simple line sources. The pressure at a given distance from the source is computed as follows:

$$p(r, t) = \left(\frac{p_0}{r}\right)^{\frac{1}{2}} \exp[j(\omega t - kr) - \alpha r] \quad (7)$$

where α is the attenuation coefficient (Np/m) and r is the radial distance from the source (m). Our simulation routine is similar to that utilized by Buchanan [7], in that they modeled the transducer as an evenly spaced array of simple sources ($a \ll \lambda$), whereas our model treats it as an ensemble of elements of finite width. More simulation results for steering can be found in our paper found elsewhere in this volume [8].

RESULTS AND DISCUSSION

A numerical simulation of the full-field acoustic pressure distribution is utilized to demonstrate some key effects of focusing within and beyond the transition range of a linear phased array. A comparison between steering and focusing is undertaken, revealing a distinct benefit of focusing over steering within the near field.

The array simulated is made up of 16 elements, with a frequency of 170 kHz, center-to-center element spacing of $\lambda/2$, and a wavespeed of 3,650 m/s . The transition range for this array is calculated to be 50 cm . The array is consistent with one that would be used for the NDE of concrete structures, but the conclusions brought forth are valid for other applications including metal applications and medical evaluation.

A directivity plot is used to show the pressure along a radial distance from the center of the array, and is an accepted standard to demonstrate the accuracy of steering and focusing behavior. An ideal plot should have a very good directivity, characterized by a very narrow main lobe width [3]. 'They are derived from the image of pressure distribution, which maps the contributions of pressure from each element via Huyghen's principle. These contributions incorporate the respective phase shifts, which lead to constructive and destructive interference of the ultrasound.

Figure 1(a) shows an image of the pressure distribution for a beam steered at 30 degrees, and Fig. 1(c) shows the directivity at $r = 20 \text{ cm}$. Since the directivity is taken in the near field of the array, the beam steering quality is quite poor, characterized by the wide and irregularly shaped main lobe. A received signal from this region could not be properly mapped to the appropriate location on an image, because the resolution of which is determined by the sharpness of the main lobe. By contrast, Fig. 1(b) shows an image pressure distribution as the beam is steered at the same angle and is also being focused at a distance $F = 20 \text{ cm}$. The directivity shown in Fig. 1(d), which passes through this focal point ($r = F$), shows a dramatic improvement over that of steering. Looking at the respective pressure distribution images, the focusing effect in the near field is quite obvious. Focusing enables the acquisition of data from within a region not previously attainable by steering only, and contributes to increased resolution capabilities within the transition zone of the array.

Referring back to eq. (5), when the focal length is infinitely large, i.e., $F \rightarrow \infty$, then $A \rightarrow -\omega\Delta\tau_0^2 + kd \sin \theta$, and $B \rightarrow 0$. In this case, it can be easily shown that the pressure distribution for focusing becomes exactly that of the steering [4]. This means that if the focal length is sufficiently large, i.e., beyond the transition range, the pressure distribution for focusing will converge to that of steering.

Figure 2 illustrates this concept. Figure 2(a) shows the pressure field of the beam steered at 30° while the corresponding directivity taken at $r = 1 \text{ m}$ is shown in Fig. 2(c). This is beyond the transition zone, and as such, the directivity is good. On the other hand, Fig. 2(b) shows the pressure field of the array now being focused in the far field at $F = 1 \text{ m}$, which now resembles that of steering. Taking a directivity at $r = F = 1 \text{ m}$, the benefit over focusing is negligible as shown in Fig. 2(d). This is critical, because this means that at the locations beyond the transition zone, the use of only steering is sufficiently adequate. Since focusing requires analysis of a large number of scanned points, it does introduce a cost, namely scanning time. Steering is much more efficient, as each sectorial line can be analyzed at a time.

Directivities are not the only criteria that should be considered when evaluating the importance of focusing. Simulating the pressure along the steered direction, Fig. 1(e) and 1(f), 2(e) and 2(f) respectively shows how the pressure of focusing compares to that of steering in the near and far fields. Within the transition range, the pressure with focusing is more concentrated than that with steering. This added pressure contribution improves the resolution when acquiring data from the near field. Figure 2(e) and 2(f) also show that beyond the transition range, the pressure along the steered direction when focusing will also converge to that of steering. This compliments the observations made analytically and utilizing the directivity plots. Figure 1 also demonstrates another important fact, that the maximum pressure does not necessarily occur at the focal point. For example, Figure 1(f) shows that the maximum pressure occurs at approximately 15 cm when the focal point is set at 20 cm . Despite the fact that the maximum pressure occurs elsewhere than the focal spot, it is important to note that the focal length is the distance that defines the best directivity.

CONCLUSION

An attempt was made to reach an analytical solution to the pressure distribution with focusing, resulting in an unclosed form. Therefore, a numerical simulation was

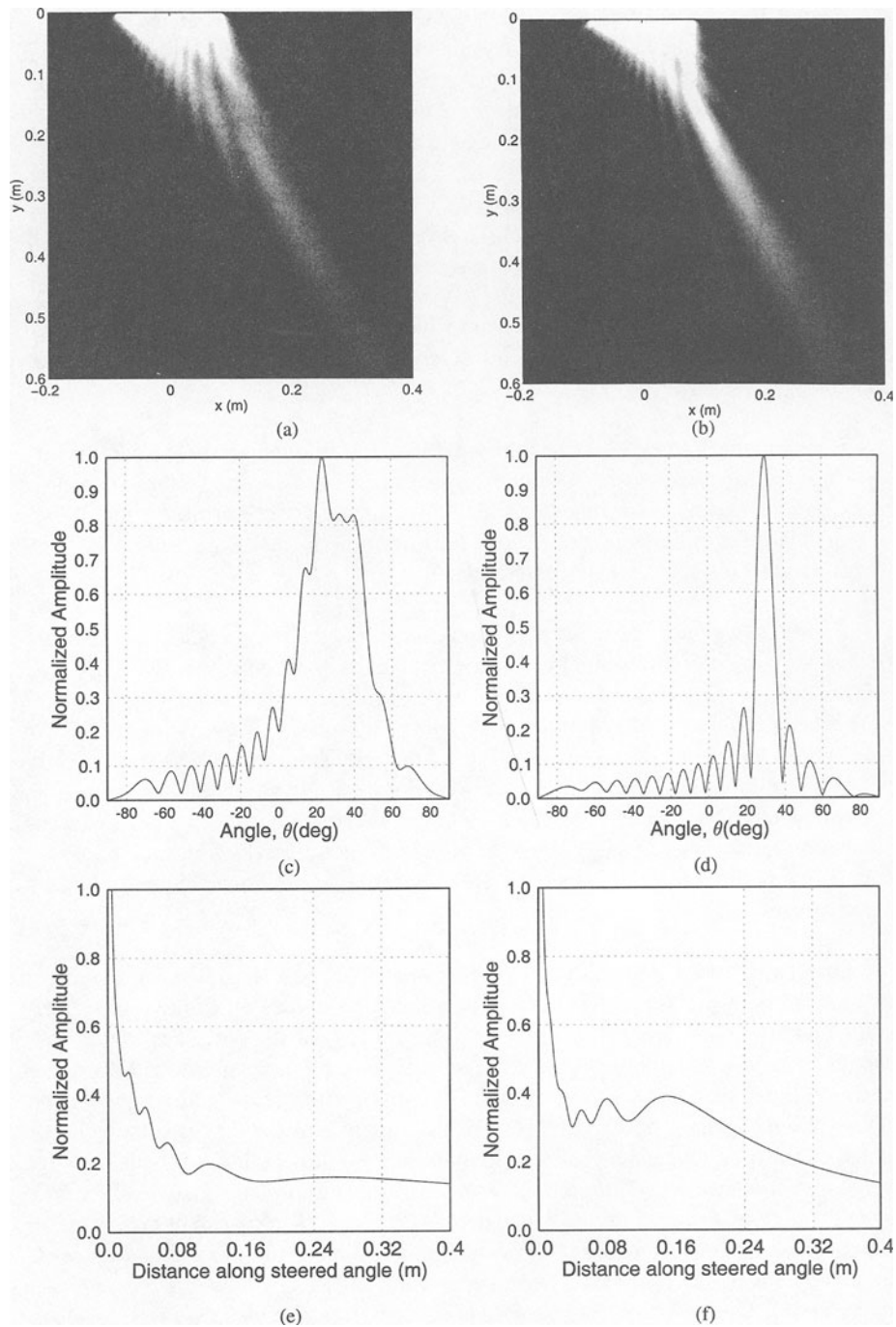


Figure 1. Comparison of beam steering (left) and focusing (right), with directivities (c, d) taken in the near field, and comparing the pressure profiles along the steered angle (e, f). ($r = 20 \text{ cm}$, $F = 20 \text{ cm}$ (focusing only), $N = 16$, $c = 3,650 \text{ m/s}$, $f = 170 \text{ kHz}$, $\theta_s = 30^\circ$, and $d = \lambda/2$).

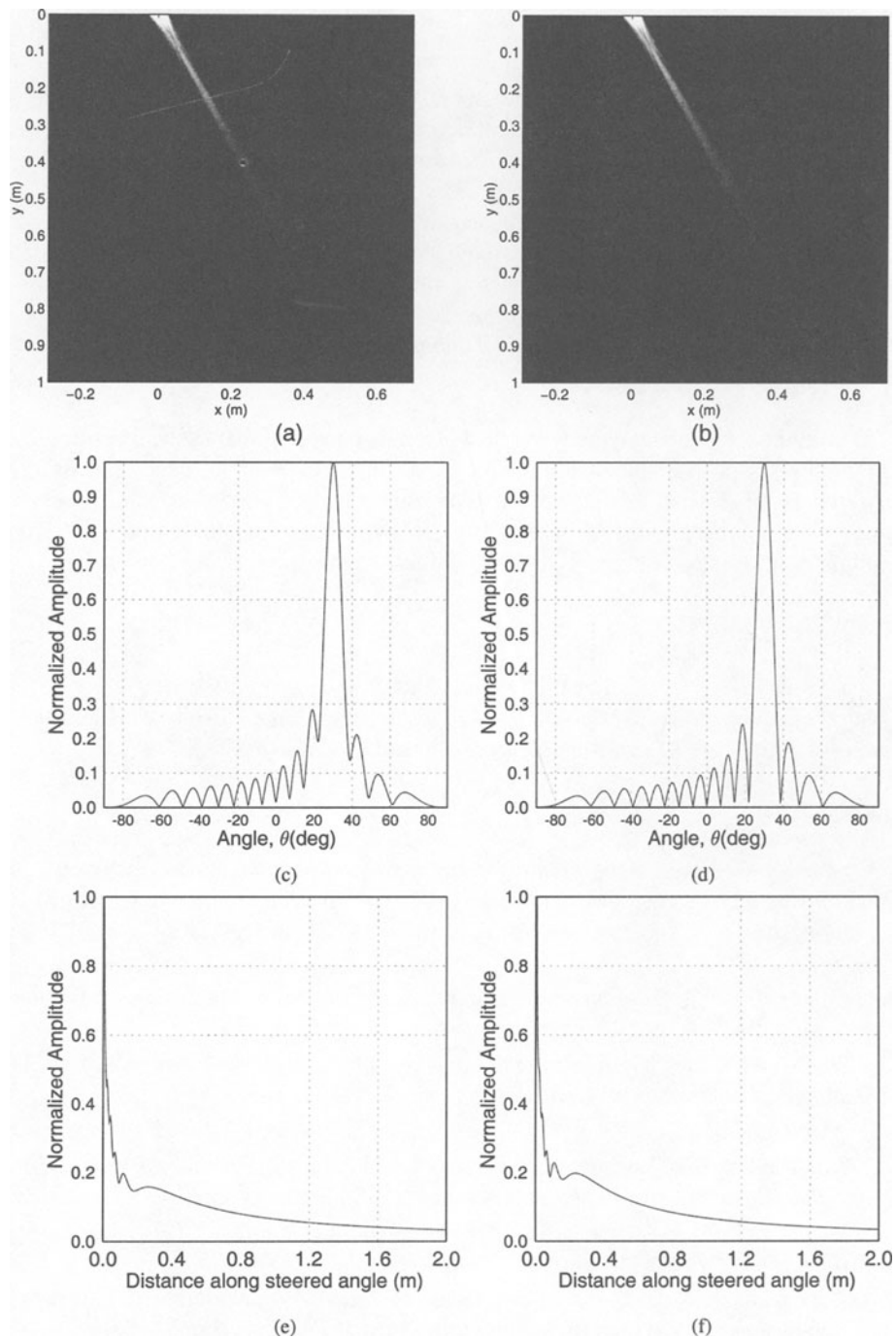


Figure 2. Comparison of beam steering (left) and focusing (right), with directivities (c, d) taken in the near field, and comparing the pressure profiles along the steered angle (e, f). ($r = 1$ m, $F = 1$ m (focusing only), $N = 16$, $c = 3,650$ m/s, $f = 170$ kHz, $\theta_s = 30^\circ$, and $d = \lambda/2$).

recommended to attain the pressure field, based on Huyghen's principle for a discrete number of simple sources.

Numerical directivity and image pressure profiles were utilized to compare the behavior of focusing and steering within, and beyond, the transition zone of the phased array. This demonstrated the importance of focusing in the near field, as the directivity for steering is quite poor, while that of focusing is very well defined. This transition range is proportional to the square of the overall dimension of the array. As the number of elements increases, there is a subsequent increase in the region where steering cannot be used. To benefit from the added number of elements, focusing must be used in this "dead" zone. Although the maximum pressure along the steered direction when focusing does not always coincide with the focal point, focusing does demonstrate better directivity at that point and an overall improvement over steering.

The numerical simulation proved our analytical conclusion that as the focal length goes to infinity, the pressure distribution of focusing converges to that of steering. This validates the use of steering beyond the transition zone, which enable faster acquisition over focusing. Although there is still some improvement beyond this zone, those improvements are negligible, since the convergence applies to a focal length approaching infinity.

ACKNOWLEDGEMENTS

This study was supported by the Korea Highway Corporation. We are grateful to Dr. Chang-Guen Lee, Program Manager and Mr. Keon-Chang Cho, Director of Highway Research Institute of the KHC, for their encouragement and support.

REFERENCES

1. L. Azar and S. C. Wooh, "A novel ultrasonic phased arrays for the nondestructive evaluation of concrete structures," in *Review of Progress in Quantitative Nondestructive Evaluation*, eds. D. O. Thompson and D. E. Chimenti, (Plenum Press, New York 1999), in this volume.
2. M. G. Silk, *Ultrasonic Transducers for Nondestructive Testing*, (Adams Hilger, Bristol, 1984).
3. S. C. Wooh, and Y. Shi, "Optimization of ultrasonic phased arrays," *Review of Progress in Quantitative Nondestructive Evaluation*, *op. cit.*, (1998), p. 883.
4. Y. Shi, *Modeling of acoustic waves for linear phased arrays*, MIT MS thesis (1998).
5. S. C. Wooh and Y. Shi, "Design Strategies for Phased Arrays," in *Review of Progress in Quantitative Nondestructive Evaluation*, *op. cit.*, (1999), in this volume.
6. O. T. Von Ramm and S. W. Smith, "Beam steering with linear arrays," *IEEE Trans. on Biomedical Engineering* BME-30, 8 (1983), p. 438.
7. M. T. Buchanan and K. Hynynen, "Design and experimental evaluation of an intracavity ultrasound phased array system for hyperthermia," *IEEE Trans. on Biomedical Engineering* 41, 12 (1994), p. 1178.
8. S. C. Wooh, and Y. Shi, "Simulated pressure field and directivity of phased arrays," *Review of Progress in Quantitative Nondestructive Evaluation*, *op. cit.*, (1999), in this volume.